Fish and Shellfish Immunology 91 (2019) 108–121

Contents lists available at ScienceDirect

Fish and Shellfish Immunology

journal homepage: www.elsevier.com/locate/fsi

Full length article

Molecular cloning and functional characterization of TRIF in large yellow croaker *Larimichthys crocea*

Peng Fei Zou[a,1], Juan Juan Shen[a,1], Ying Li[b], Qingpi Yan[a], Zhi Hua Zou[a], Zi Ping Zhang[c], Yi Lei Wang[a,*]

[a] College of Fisheries, Jimei University, Xiamen, Fujian Province, 361021, China
[b] Key Laboratory of Estuarine Ecological Security and Environmental Health, Tan Kah Kee College, Xiamen University, Zhangzhou, Fujian Province, 363105, China
[c] College of Animal Science, Fujian Agriculture and Forestry University, Fuzhou, Fujian Province, 350002, China

ARTICLE INFO

Keywords:
Toll-like receptor
TRIF
NF-κB
Type I IFN
Large yellow croaker

ABSTRACT

As an adaptor in Toll-like receptor (TLR) signaling pathway, Toll/interleukin-1 receptor (TIR) domain containing adaptor inducing interferon-β (TRIF) mediates downstream signaling cascades and plays important roles in host innate immune responses. In the present study, a TRIF ortholog named *Lc*-TRIF was identified in large yellow croaker (*Larimichthys crocea*). Sequence comparison analysis revealed that *Lc*-TRIF has a conserved TIR domain but without TRAF6 binding motif. The genome structure of *Lc*-TRIF is conserved, with two exons and one intron. Syntenic comparison showed that the loci of fish TRIF was different from that in mammals or birds, and TRAM was absent in the genomes of fish, amphibians, and birds, but present in mammals and reptiles. Expression analysis revealed that *Lc*-TRIF was broadly expressed in examined organs/tissues, with the highest expression level in gill and weakest in brain, and could be up-regulated under poly I:C, LPS, PGN, and *Pseudomonas plecoglossicida* stimulation. Fluorescence microscopy results showed that *Lc*-TRIF exhibited a global localization throughout the entire cell including the nucleus in HEK 293T cells. Additionally, luciferase assays demonstrated that *Lc*-TRIF expression could significantly induce NF-κB, type I IFN, IRF3 as well as IRF7 promoter activation. These results collectively indicated that *Lc*-TRIF was function in host antiviral and antibacterial responses via NF-κB and IRF3/7 related signaling pathway.

1. Introduction

The innate immune system is the first line of host defense against bacterial and viral infection, which is initiated by host pattern recognition receptors (PRRs) that recognize specific molecular structures from invading microorganisms known as pathogen-associated molecular patterns (PAMPs) and also host danger signals named danger-associated molecular patterns (DAMPs) [1–4]. To date, five major classes based on protein domain homology of PRRs have been identified and investigated, including Toll-like receptors (TLRs), retinoic acid inducible gene I (RIG-I)-like receptors (RLRs), nucleotide-binding oligomerization domain (NOD)-like receptors (NLRs), C-type lectin receptors (CLRs) and absent in melanoma 2 (AIM2)-like receptors (ALRs) [2,5,6].

The functional characterization of TLRs was intensively studied during the past decades, with 10 and 12 functional TLRs have been identified in human and mice (TLR1-10 in human, TLR1-9, TLR11-13 in mice), respectively [3,4]. Interestingly, TLRs in bony fish have some unique members that called “fish-specific” TLRs, such as TLR19, TLR20, TLR21, TLR22, and TLR23 [7,8]. TLRs mediated signaling cascade involves a number of adaptors, which trigger downstream protein kinases that leading to the activation of transcription factors including nuclear factor-κB (NF-κB) and interferon (IFN)-regulatory factor (IRF) family [9,10]. So far, five important adaptors of TLRs have been identified, including myeloid differentiation primary response 88 (MyD88), Toll-interleukin 1 receptor (TIR) domain-containing adapter protein (TIRAP, also known as MyD88-adaptor-like, MAL), TIR-domain-containing adaptor protein inducing IFNβ (TRIF, also known as Toll-like receptor adaptor molecule 1, TICAM1), TRIF-related adaptor molecule (TRAM, also known as TICAM2) and sterile α- and armadillo-motif-containing protein (SARM) [11,12].

TRIF, as an adaptor of TLR3 and TLR4, play an important role in TLR3-and TLR4-mediated signaling pathway in mammals [2,4]. During TLR3-mediated pathway, TRIF is responsible for initiating the signaling cascade in which tumor necrosis factor (TNF) receptor-associated factor

* Corresponding author.
E-mail address: ylwang@jmu.edu.cn (Y.L. Wang).
[1] Both authors have the same contribution.

https://doi.org/10.1016/j.fsi.2019.05.011
Received 1 February 2019; Received in revised form 3 May 2019; Accepted 6 May 2019
Available online 12 May 2019

Table 1
Primer sequences used in this study.

Primer name	Sequence (5′–3′)	Application
Lc-TRIF-F	ATGAGCCGCGAGGGAGAAGA	*Lc*-TRIF ORF cloning
Lc-TRIF-R	CTATTGCTCATCTAAATCATCT	
Lc-TRIF-5-R1	AGTTTGTTCAGGGCCTCCGTCT	PCR for 5′ RACE
Lc-TRIF-5-R2	CAGTCGCTCCTGAGGTGCTTTA	PCR for 5′ RACE
Lc-TRIF-3-F1	TGTCCCAATGTGCCACCAGAAC	PCR for 3′ RACE
Lc-TRIF-3-F2	GGGTTGGGTGGAGGTGAAGACA	PCR for 3′ RACE
ALOP	GGCCACGCGTCGACTAGTACT(16)(A/C/G)	General primers for RACE
AP	GGCCACGCGTCGACTAGTAC	
AAP	GGCCACGCGTCGACTAGTACGGGGGGGGGG	
Lc-TRIF-G-F	TGCTGTGCAAAAGTGTTTGAAGC	PCR for genomic cloning
Lc-TRIF-G-R	TTGTCACGGGAGATGGGAAATA	
pcDNA3.1-TRIF-F	CCGCTCGAGCGATGGCTAGCCGCGAGGGAGAAGA	pcDNA3.1-TRIF
pcDNA3.1-TRIF-R	CGGGGTACCTTGCTCATCTAAATCATCT	
pTurbo-TRIF-F	CCGCTCGAGATGGCTAGCCGCGAGGGAGAAGA	pTurbo-TRIF-GFP
pTurbo-TRIF-R	CGGGGTACCGTTTGCTCATCTAAATCATCT	
qTRIF-F	CACTCGATGAGAGCAGGAGCTTT	Quantitative real-time PCR
qTRIF-R	GTTCTGGTGGCACATTGGGAC	
qβ-actin-F	TTATGAAGGCTATGCCCTGCC	Quantitative real-time PCR
qβ-actin-R	TGAAGGAGTAGCCACGCTCTGT	

3 (TRAF3) and TRAF family member-associated NF-κB activator (TANK) act as a bridge to the activation of TANK-binding kinase 1 (TBK1), which lead to direct phosphorylation of IRF3 and IRF7 and then promote IFN and IFN-inducible genes production. Whereas in TLR4-mediated pathway, another adaptor TRAM is needed to connect TLR4 and TRIF, and then TRIF-TRAF3-TBK1-IRF3/7 signaling cascade could be activated [9,12,13]. In addition, TRIF-dependent activation of NF-κB is also been induced downstream of TLR3-and TLR4-mediated signaling, in which receptor interacting protein 1 (RIP1) and TRAF6 are recruited and then activate transforming growth factor-activated protein kinase 1 (TAK1), resulting in IκB kinase (IKK)-mediated NF-κB activation as well as activation of mitogen-activated protein kinase (MAPK) pathway, which play central roles in induction of cytokines and chemokines production in proinflammatory response [9,12,13].

In addition to the functional investigation of TRIF in mammals, homologs of TRIF have also been cloned and identified in teleost fish, such as channel catfish (*Ictalurus punctatus*) [14], zebrafish (*Danio rerio*) [15,16], fugu (*Takifugu rubripes*) [17], grass carp (*Ctenopharyngodon idella*) [18], and orange-spotted grouper (*Epinephelus coioides*) [19]. Intriguingly, it has been revealed that fugu have two arms of TRIF pathway evolved as dsRNA receptors, TLR3 and TLR22 (a “fish-specific” TLR), which could form a complex with TRIF, with TLR22 function in the antiviral signaling [17,20], suggesting that fish TRIF-mediated signaling pathway function importantly in fish immune response.

In the present study, ortholog of mammalian TRIF was cloned and identified in large yellow croaker, *Larimichthys crocea*, named *Lc*-TRIF. The comparison of protein sequence of *Lc*-TRIF with other known TRIF proteins and phylogenetic relationship were analyzed, and the genome organization, the expression patterns of *Lc*-TRIF in different organs/tissues as well as stimulation under various PAMPs or bacterial pathogen were also determined. In addition, the subcellular localization and the induction of *Lc*-TRIF in the activation of NF-κB, type I IFN, IRF3 and IRF7 were also detected. Hence the present research provides perspectives into the functional characterization of teleost TRIF, which may be of great importance in understanding the function of TRIF in vertebrates.

2. Materials and methods

2.1. Fish, cell lines and transfection

Large yellow croaker with length 18 ± 1.5 cm, weight 60 ± 15 g that used in this study were purchased from Ningde Fufa Fishing Co., Ltd, Ningde, Fujian Province, China. The fish were kept in laboratory recirculating seawater systems for 2 weeks before use.

Human embryonic kidney 293T (HEK 293T) cells were cultured as described previously [21–23]. Briefly, HEK 293T cells were cultured in Dulbecco modified Eagle medium (DMEM) at 37 °C with 5% CO_2, 10% fetal bovine serum (FBS, Invitrogen-Gibco) and 100 U/ml penicillin (P) and streptomycin (S). Transfection of plasmids in HEK 293T cells were performed using Lipofectamine 3000 (Invitrogen, Carlsbad, CA) according to manufacturer's instructions.

2.2. Gene expression patterns assay

To understand the tissue distribution pattern of TRIF in large yellow croaker, organs/tissues including gill, liver, spleen, head kidney, kidney, intestine, heart, brain, skin, muscle, and blood were dissected from 6 healthy fish with anaesthetization in 0.01% eugenol and then put into liquid nitrogen immediately for RNA extraction.

To evaluate the expression pattern of TRIF under different immune stimulation, the fish were divided into five groups and injected with different PAMPs and bacterium. In brief, each fish of challenge groups was injected intraperitoneally with 100 μl suspension of *Pseudomonas plecoglossicida* (5×10^5 CFU/ml) in phosphate buffered saline (PBS) [24,25], 100 μl lipopolysaccharides (LPS) (L3024, Sigma, from *Escherichia coli* O111:B4, 0.5 mg/ml), 100 μl peptidoglycan (PGN) (69554, Sigma, from *Bacillus subtilis*, 1 mg/ml) or 100 μl polyinosinic-polycytidylic acid potassium salt (poly I:C) (P9582, Sigma, 1 mg/ml) in PBS [26], respectively. And fish of the control group was injected with the same volume of PBS. At 3, 6, 12 and 24 h post injection (hpi), 6 fish from each group were anaesthetized in 0.01% eugenol, and different organs/tissues including gill, head kidney, spleen, intestine, and blood were collected for RNA extraction.

2.3. Gene cloning and plasmids construction

Total RNA was extracted using TRIzol® Reagent (Invirtogen) from the organs/tissues samples described above according to manufacturer's instructions. 1 μg total RNA was treated with RNase-free DNase I (Thermo Scientific™) and then reverse-transcribed using a first-stand cDNA synthesis kit (RevertAid First Stand cDNA Synthesis Kit, #K1622, Thermo Scientific™) following the manufacturer's protocol. The synthetic cDNA was then kept at −20 °C and used as a template for open reading frame (ORF) cloning of target genes or quantitative real-time PCR (qRT-PCR) analysis.

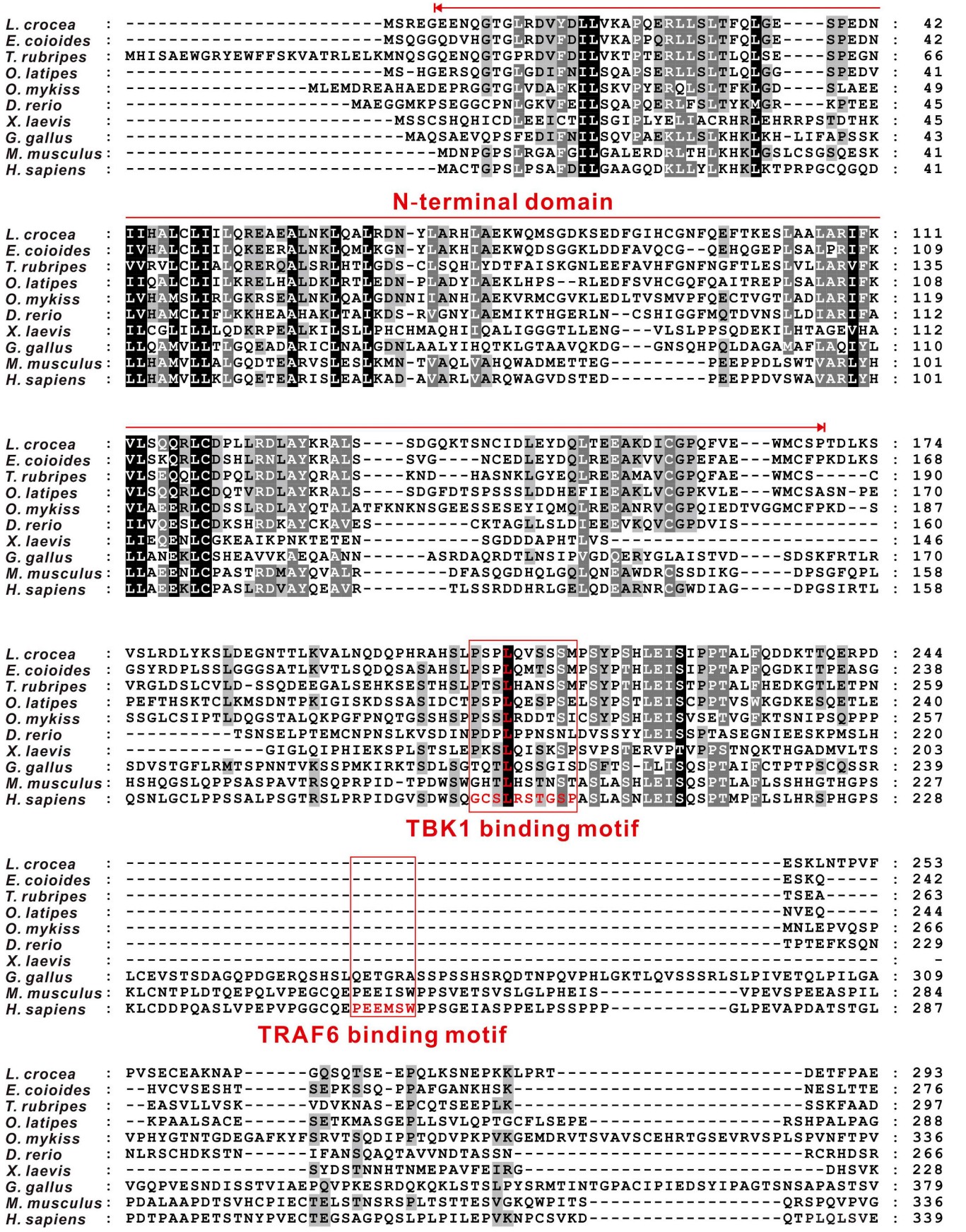

(caption on next page)

Fig. 1. Multiple alignment of the protein sequence of *Lc*-TRIF with their counterparts in other vertebrates. Sequences shaded in black are positions where all the sequences share the same amino acid residue, whereas those shaded in gray and light gray represent conservative and semi-conservation amino acid substitutions, respectively. TIR (Toll/interleukin-1 receptor) domain is indicated with black arrows. The N-terminal domain, C-terminal RHIM domain, TBK1 and TRAF6 binding motifs determined in mammals are indicated with red arrows and boxes, respectively, with the sequence of RHIM domain, TBK1 and TRAF6 binding motifs in human marked with red, and the conserved Leu in TBK1 binding motif in all detected vertebrates is also presented in red. (For interpretation of the references to colour in this figure legend, the reader is referred to the Web version of this article.)

To obtain the full-length cDNA of large yellow croaker TRIF, the partial sequence was obtained by PCR with specific primers designed based on the data in NCBI GenBank database (Accession No. XM_010738293.3), and the 3′ and 5′ UTRs were obtained by 3′ and 5′ RACE, respectively. The first-strand cDNA used as a template for 3′ RACE was synthesized using AOLP primer, and that for 5′ RACE was synthesized using AAP and oligo(dT)$_{18}$ primer following the manufacturer's protocol. Nested primers *Lc*-TRIF-3-F1 and *Lc*-TRIF-3-F2 were designed and used in combination with the adaptor primer AP for 3′ RACE, whereas nested primers *Lc*-TRIF-5-R1 and *Lc*-TRIF-5-R2 together with AP primer were used for 5′ RACE (Table 1). The PCR products were cloned into pMD19-T vector (Takara, Dalian, China) for sequencing by Sangon Biotech Co., Ltd (Shanghai, China).

The genomic sequence of large yellow croaker TRIF was amplified by using gene-specific primer *Lc*-TRIF-G-F and *Lc*-TRIF-G-R (Table 1) using genomic DNA extracted from muscle as a template. PCR was performed using LA-Taq (Takara, Dalian, China) as follows: 1 cycle of denaturalization at 94 °C for 3 min, 35 cycles of denaturalization at 94 °C for 30 s, annealing at 56 °C for 30 s and extension at 72 °C for 3 min, followed by a final extension at 72 °C for 10 min. The PCR products were purified, cloned and sequenced as described above.

For eukaryotic expression, the ORF of large yellow croaker TRIF was subcloned into pcDNA3.1/*myc*-His (−) A vector (Invitrogen, Carlsbad, CA). For subcellular localization assays, the entire ORF of TRIF was inserted into pTurboGFP-N vector (Evrogen, Moscow, Russia). All plasmid constructs were verified by sequencing analysis. The primers with the restricted enzyme cutting sites were listed in Table 1.

2.4. Bioinformatics analysis

Protein sequence prediction was performed using software at the ExPASy Bioinformatics Resource Portal (http://www.expasy.org/proteomics), with conserved domain structures detected by using the Conserved Domain Database (CDD) on NCBI (http://www.ncbi.nlm.nih.gov/cdd) [27]. Vertebrates TRIF as well as TRAM were searched with the Basic Local Alignment Search Tool (BLAST) analysis tool of National Center for Biotechnology information website (NCBI, http://blast.ncbi.nlm.nih.gov/Blast.cgi). Multiple alignments of amino acids (aa) sequences were generated in CLUSTAL X [28] and the results were subsequently edited by using GeneDoc program. Phylogenetic tree was constructed using the Neighbor-Joining method in MEGA 7 software [29]. Vertebrates genomes of TRIF were searched on NCBI genome database (https://www.ncbi.nlm.nih.gov/genome/), followed by analysis online using Splign (https://www.ncbi.nlm.nih.gov/sutils/splign/splign.cgi). Systematic searches for vertebrates TRIF and TRAM loci were performed using the BLAST program and BioMart in Ensembl (http://www.ensembl.org/) and NCBI genome database.

2.5. Fluorescence microscopy

To detect the subcellular localization of large yellow croaker TRIF, HEK 293T cells were passaged and cultured into 6-well plates with 1×10^6 cells per well overnight. After that, 5 μg of plasmid constructs of pTurbo-TRIF-GFP and pTurboGFP-N (vector control) were transfected into the cells using Lipofectamine 3000, respectively. Approximately 24 h post-transfection (hpt), HEK 293T cells were stained with Hoechst 33342 (Sigma-Aldrich, St Louis, MO), before being examined and photographed under a fluorescent microscope (Leica, Germany). Additionally, the cells were subsequently collected for determination of TRIF-GFP and pTurboGFP fusion proteins using western blotting analysis, with the primary antibody (*Anti*-TurboGFP antibody, Evrogen, CAT. #AB513) diluted at 1:5000. The bands were detected by using WesternBright™ ECL HRP substrate (Advansta, San Jose, USA) and ECL western blotting system (LAS-4000mini, Fujifilm, Tokyo, Japan) according to manufacturers' instructions.

2.6. qRT-PCR

qRT-PCR was performed using Go Taq® qPCR Master Mix (Promega, Madison, USA) on a Roche LightCycler® 480 II quantitative real-time detection system (Roche, Switzerland). PCR amplifications were carried out under the following conditions: 5 min at 95 °C, followed by 40 cycles of 20 s at 95 °C, 15 s at 56 °C and 15 s at 72 °C, then with melting curve analysis of the products by raising the temperature with 0.5 °C per second from 65 °C up to 95 °C. All reactions were performed in triplicate in a 384 well plate, with the mean value recorded. The relative expression of target genes was normalized to the expression of β-actin and analyzed using the comparative Ct method ($2^{-\Delta\Delta Ct}$) [30]. Statistical analysis was conducted using one way ANOVA by SPASS 16.0 and a probability level of $P < 0.05$ or $P < 0.01$ was considered as statistically significant. All primers used for qRT-PCR are listed in Table 1.

2.7. Luciferase activity assay

To determine the effect of large yellow croaker TRIF on the NF-κB, IFN, IRF3, and IRF7 activity, HEK 293T cells seeded overnight in 24-well plates at 1×10^5 cells per well were transiently transfected with 100 ng of pNF-κB-luc (Clontech, Palo Alto, CA), pGL4-IFN1-pro (application number: 201710456729.3), pGL4-IRF3-pro (application number: 201710457836.8) or pGL4-IRF7-pro (application number: 201710457820.7), 10 ng pRL-TK (Promega, Madison, WI) together with increasing concentrations of pcDNA3.1-TRIF (5, 10, 50, 100, and 200 ng) or pcDNA3.1 empty vector with the same concentrations (control) using Lipofectamine 3000. At 24 hpt, the cells were harvested and lysed using Dual-Luciferase Reporter System (Promega) according to the manufacture's instructions. Luciferase activities were measured by a Promega GloMax® 20/20 luminometer (Promega), data were normalized to the *Renilla* luciferase activities and expressed as the fold stimulation relative to control group transfected with empty vector. All values were expressed as mean of three independent experiments, and statistical analysis was conducted using one way ANOVA as described above with a probability level of $P < 0.05$ or $P < 0.01$ was considered as statistically significant.

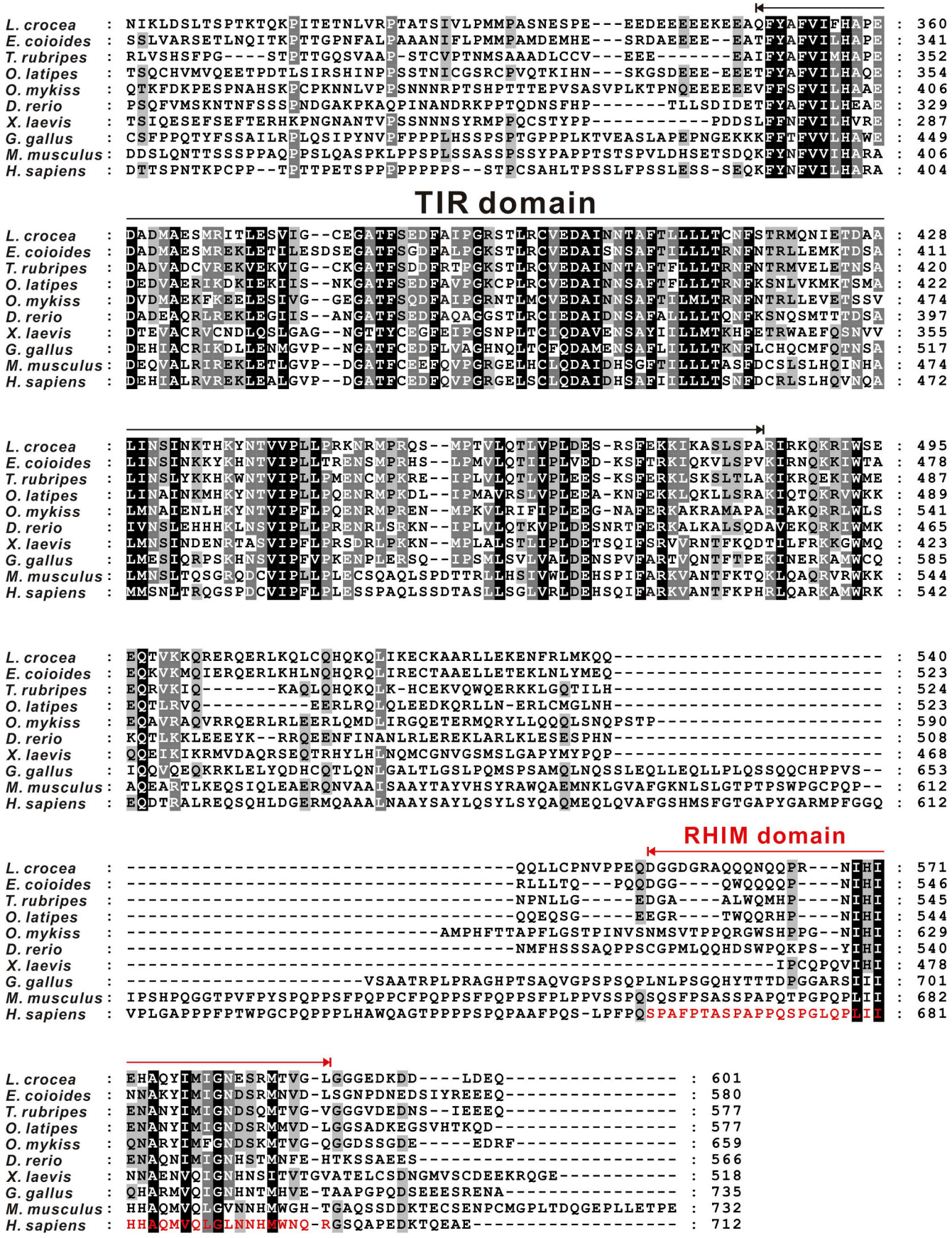

Fig. 1. (*continued*)

Table 2
Amino acid identity and similarity among *Lc*-TRIF and TRIF from other vertebrates.

Common name	Scientific name	Accession No.	Length (aa)	Identity	Similarity
Grouper	*Epinephelus coioides*	AEX01719.1	580	59%	73%
Fugu	*Takifugu rubripes*	NP_001106665.1	577	46%	61%
Medaka	*Oryzias latipes*	XP_011485063.1	577	44%	61%
Rainbow trout	*Oncorhynchus mykiss*	XP_021454523.1	659	38%	54%
Zebrafish	*Danio rerio*	ABP04048.1	566	28%	45%
African clawed frog	*Xenopus laevis*	XP_018109628.1	518	17%	34%
Chicken	*Gallus gallus*	NP_001074975.1	735	18%	34%
Mouse	*Mus musculus*	NM_174989.4	732	18%	34%
Human	*Homo sapiens*	AB093555.1	712	19%	33%

3. Results

3.1. Sequence analysis of TRIF in large yellow croaker and other vertebrates

The identified ortholog of TRIF in large yellow croaker, named as *Lc*-TRIF (GenBank accession No. MK863372) was 2834 bp, with an ORF of 1806 bp encoding a protein of 601 amino acids (aa) (Supplemental Fig. 1), and that was smaller than orthologs identified in mammals (mouse TRIF, 732 aa; human TRIF, 712 aa). Using NCBI CDD, it was found that *Lc*-TRIF contained a conserved TIR domain (Fig. 1).

Multiple alignments and amino acid sequence similarity comparison of *Lc*-TRIF with TRIF in other fishes, amphibian, birds, and mammals, including grouper (*Epinephelus coioides*), fugu (*Takifugu rubripes*), medaka (*Oryzias latipes*), rainbow trout (*Oncorhynchus mykiss*), zebrafish (*Danio rereio*), African clawed frog (*Xenopus laevis*), chicken (*Gallus gallus*), mouse (*Mus musculus*), and human (*Homo sapiens*) were shown in Fig. 1, which revealed a relatively conserved TIR domain in fish, amphibian, birds and mammals, whereas orthologs in fish and amphibian exhibited significant gaps in the N and C terminal of the protein sequences when compared with that in birds and mammals. Furthermore, no identifiable TRAF6 binding motif (positions 250–255 in human) was found in fish or amphibian. Some sequence divergence was also noted in the N-terminal domain (consensus positions 1–153 in human), TBK1 binding motif (positions 191–200 in human) and C-terminal RIP homotypic interaction motif (RHIM) (positions 661–699 in human). Interestingly, the Leu^{194} mentioned in TBK1 binding motif of TRIF in human was highly conserved in all detected vertebrates. Additionally, the protein sequence of *Lc*-TRIF has a similarity of 73% with TRIF of grouper, 61% with fugu, 61% with medaka, 54% rainbow trout, and 45% with zebrafish, exhibiting a relatively strong homology among different fishes, whereas such similarity level went down when compared with TRIF in amphibian, birds, and mammals, with a similarity of 34% to that in African clawed frog, chicken, and mouse, and 33% in human (Table 2).

To determine the phylogenic relationship of TRIF in vertebrates, a phylogenetic tree including orthologs of five TIR-domain-containing adaptors (TRIF, TRAM, TIRAP, MyD88 and SARM) in TLR signaling was constructed using protein sequences based on neighbor-joining method (Fig. 2). The results showed that *Lc*-TRIF was clustered to its corresponding members of TRIF family. Five branches originated from the tree represented the distinct TRIF, TRAM, TIRAP, MyD88, and SARM families. The members of TRIF family from different fishes were clustered as one clade, and that from amphibians, birds, reptiles, and mammals were grouped into another clade in the TRIF family. In addition, the members of the TRIF and TRAM families form a monophyletic group with a high level of 99% bootstrap support, and then clustered with TIRAP and MyD88 family, with members of SARM family exhibited a long evolutionary distance from the TRIF family in the five TLR adaptors. Interestingly, no fish orthologs of TRAM has been detected, even in amphibians or birds (Fig. 2).

3.2. Genomic organization of TRIF genes in vertebrates

The identified genomic DNA sequence of *Lc*-TRIF was 2966 bp long. By searching other vertebrate genomic sequences of TRIF genes in ENSEMBL and NCBI databases, the comparison of genomic organization among *L. crocea, D. rerio, I. punctatus, M. musculus,* and *H. sapiens* was generated. The results showed that the genomic organization of TRIF in *L. crocea* was composed of two exons and one intron as revealed from the alignment of cDNA sequence with the corresponding genomic sequence, with the coding region located in the second exon, which was similar to that found in *D. rerio*, *I. punctatus*, *M. musculus*, and *H. sapiens* (Fig. 3). Although such genomic arrangement was quite similar among the detected species, the length of the exons and introns were different from each other, especially the size of introns, which was longer in mammals than that of fishes, and *L. crocea* has the smallest size of intron with 132 bp, whereas *H. sapiens* has the largest with 13097 bp (Fig. 3).

3.3. Synteny analysis of TRIF and TRAM gene loci in vertebrates

In order to gain an insight into whether the genes surrounding TRIF and TRAM are evolutionary conserved, gene neighborhood analysis was performed to assay the conserved gene synteny in the region encoding TRIF or TRAM in fish, amphibians, birds, reptiles, and mammals. In large yellow croaker, TRIF was flanked with CCL20 and CAMSAP2 at upstream and downstream, respectively. And at least 12 genes upstream and 8 genes downstream on both sides of CCL20-TRIF-CAMSAP2 segment were arranged in the same order and transcribed in the same direction within the fish species belong to the Percomorpha and Atherinomorpha, such as *T. rubripes* and *O. latipes* (Fig. 4). However, TRIF loci was completely different in the fish species of Cyprinomorpha, birds, and mammals, which was flanked with UHRF1 and TIMM44 in *I. punctatus* and *D. rerio*, with PLIN3 and FEM1A in *G. gallus*, *M. musculus,* and *H. sapiens* at upstream and downstream, respectively. The gene synteny around TRIF was remarkably conserved in birds and mammals. Interestingly, in the series Cyprinomorpha, 5 conserved neighbouring genes were present in the TRIF locus compared with that found in birds and mammals, including PTPRS, KDM4B, UHRF1, MYDGF, and TNFAIP8L1 (Fig. 4), suggesting that chromosome block recombination might have occurred in the divergence of fish species and their vertebrate ancestors, especially in the clade of Percomorpha and Atherinomorpha.

Surprisingly, TRAM gene was only found in the genomes of

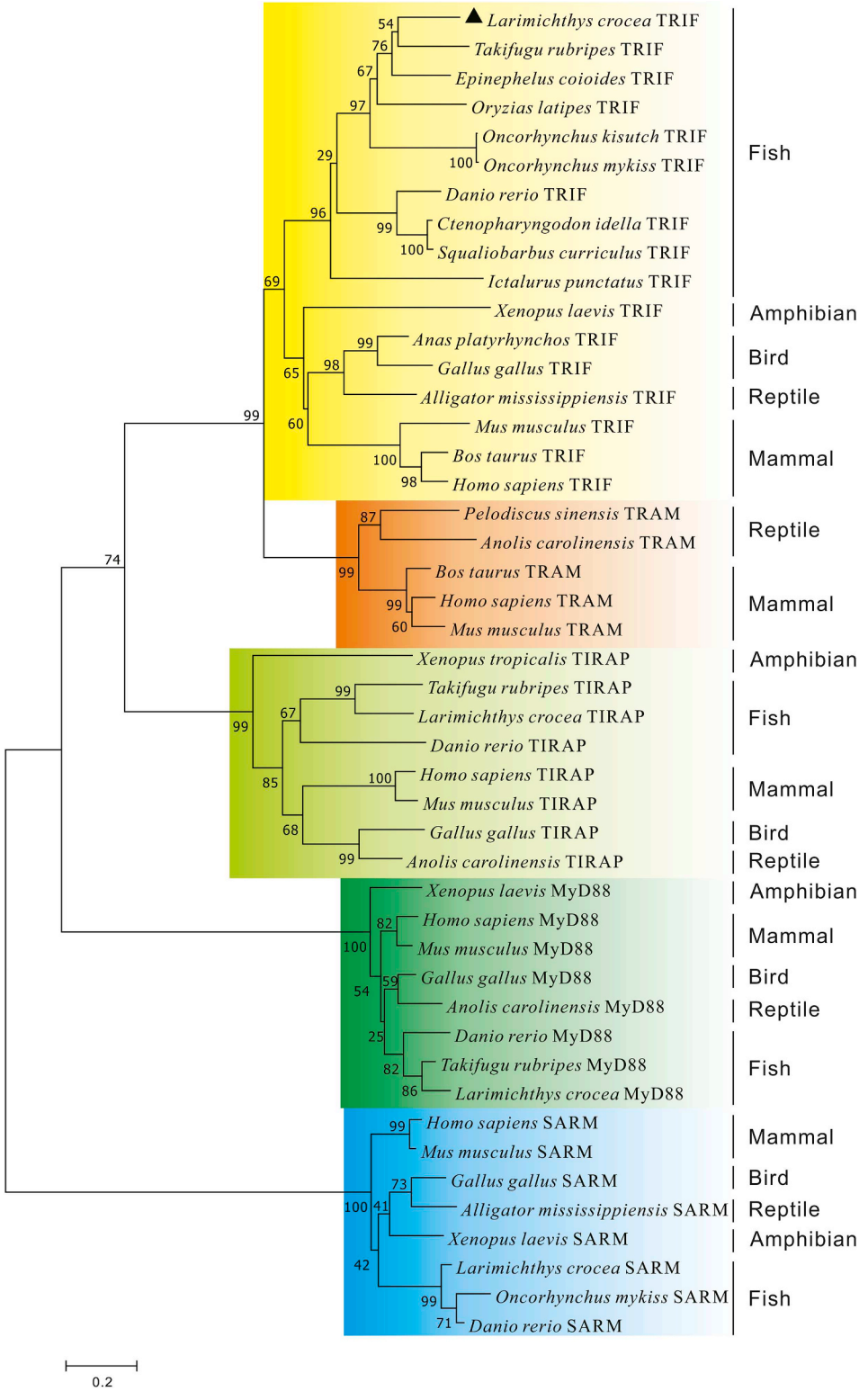

Fig. 2. Phylogenetic analysis of vertebrate TRIF, TRAM, TIRAP, MyD88, and SARM families. The phylogenetic tree was obtained by MEGA7 program using neighbor-joining method based on the amino acid sequences. The percentage of replicate trees in which the associated taxa clustered together are shown next to the branches based on 10000 replications in the bootstrap test. Block with yellow, orange, light green, green, and blue indicates group of TRIF, TRAM, TIRAP, MyD88, and SARM in vertebrates, respectively. And the subgroup of the vertebrates that the clustered TRIF, TRAM, TIRAP, MyD88 or SARM derived from are marked on the right. The GenBank accession numbers for the amino acid sequences used are as the followings: *L. crocea* TRIF, MK863372; *T. rubripes* TRIF, NP_001106665.1; *E. coioides* TRIF, AEX01719.1; *O. latipes* TRIF, XP_011485063.1; *Oncorhynchus kisutch* TRIF, XP_020347942.1; *O. mykiss* TRIF, XP_021454523.1; *I. punctatus* TRIF, NP_001187154.1; *D. rerio* TRIF, ABP04048.1; *C. idella* TRIF, AGW25589.1; *Squaliobarbus curriculus* TRIF, AMP81962.1; *Anas platyrhynchos* TRIF, NP_001297720.1; *G. gallus* TRIF, ABK20148.1; *Alligator mississippiensis* TRIF, XP_014460416.1; *M. musculus* TRIF, NM_174989.4; *Bos taurus* TRIF, NM_001030301.1; *H. sapiens* TRIF, AB093555.1; *X. laevis* TRIF, XP_018109628.1; *Pelodiscus sinensis* TRAM, XM_014579222.1; *Anolis carolinensis* TRAM, XP_016850341.1; *B. taurus* TRAM, NP_001039921.1; *H. sapiens* TRAM, NP_067681.1; *M. musculus* TRAM, NP_775570.1; *H. sapiens* TIRAP, NP_001305705.1; *M. musculus* TIRAP, NP_473437.2; *G. gallus* TIRAP, NP_001020000.1; *A. carolinensis* TIRAP, XP_008116469.1; *Xenopus tropicalis* TIRAP, NP_001037925.1; *D. rerio* TIRAP, XP_017207577.1; *T. rubripes* TIRAP, BAF91190.1; *L. crocea* TIRAP, XP_010755418.1; *H. sapiens* MyD88, NP_001166038.2; *M. musculus* MyD88, NP_034981.1; *G. gallus* MyD88, NP_001026133.2; *A. carolinensis* MyD88, XP_003221916.1; *X. laevis* MyD88, AAG10073.1; *D. rerio* MyD88, NP_997979.2; *T. rubripes* MyD88, NP_001106666.1; *L. crocea* MyD88, XP_010751574.1; *H. sapiens* SARM, NP_055892.2; *M. musculus* SARM, NP_001161993.1; *G. gallus* SARM, XP_415814.4; *A. mississippiensis* SARM, KYO40867.1; *X. laevis* SARM, XP_018101625.1; *L. crocea* SARM, XP_010734094.3; *O. mykiss* SARM, XP_021443503.1; *D. rerio* SARM, NP_001124068.1. (For interpretation of the references to colour in this figure legend, the reader is referred to the Web version of this article.)

mammals and reptiles, such as *H. sapiens*, *M. musculus*, *Anolis carolinensis,* and *Pelodiscus sinensis*, with a conserved gene synteny in the region encoding TRAM, which was located between FEM1C and TMED7, with FEM1C, CCDC112, PGGT1B, and TRIM36 upstream, and TMED7, CDO1, ATG12, AP3S1, LVRN, COMMD10, and SEMA6A downstream (Fig. 5). By analyzing genomes of amphibians, birds, and teleost fish, it appears that their genomes lack TRAM gene, which was not due to poor genome analysis, since the regions of the TRAM locus were in good quality, and such conserved gene could also been identified, only without TRAM been found between FEM1C and TMED7. Although the gene arrangement as well as the transcription direction in *L. crocea*, *T. rubripes*, *O. latipes*, *I. punctatus*, and *G. gallus* was not like that found in mammals and reptiles (Fig. 5).

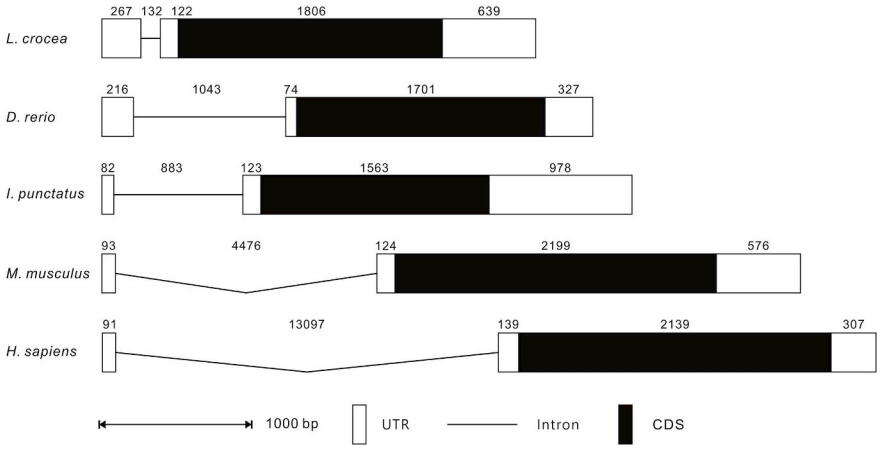

Fig. 3. Schematic comparison of *Lc*-TRIF genomic organization with other vertebrates TRIF genes. The genomic organizations of TRIF genes were compared among different species, such as *L. crocea*, *D. rerio*, *I. punctatus*, *M. musculus*, and *H. sapiens*. Exons and introns are shown by boxes and lines, with black boxes indicating the coding sequences (CDS), the white boxes representing the untranslated region (UTR), and the horizontal lines denoting the introns, respectively. The lengths in base pairs (bp) are shown above the boxes and lines with the corresponding sizes (bp) which can refer to the scale below (except for the lengths of introns in *M. musculus* and *H. sapiens*).

3.4. Subcellular localization of Lc-TRIF

To identify the subcellular localization of *Lc*-TRIF, the ORF of *Lc*-TRIF was subcloned into pTurboGFP-N expression vector. The fluorescent microscopy revealed that pTurbo-TRIF-GFP fusion protein was located throughout the entire cell including the nucleus. Additionally, control cells transfected with empty pTurboGFP-N vector showed a global cytosolic localization as well as the nucleus (Fig. 6A). The expression of pTurbo-TRIF-GFP as well as pTurboGFP fusion proteins were also confirmed using a polyclonal antibody against the TurboGFP protein by western blotting analysis, and the recombinant TRIF-GFP and pTurboGFP (control) showed correct molecular weights as revealed by *anti*-TurboGFP antibody (Fig. 6B).

3.5. Expression analysis of Lc-TRIF in organs/tissues and challenged with PAMPs

Constitutive expression pattern of *Lc*-TRIF in different organs/tissues of healthy large yellow croaker was determined based on qRT-PCR analysis. The results showed that *Lc*-TRIF was expressed in all the detected organs/tissues of the healthy fish, with the highest expression level in gill, followed by in kidney, head kidney, spleen, muscle, skin, liver, blood, intestine, heart, and the lowest expression level in brain (Fig. 7).

To further understand the expression profiles of *Lc*-TRIF during bacterial and viral infection, the temporal expression levels of *Lc*-TRIF in gill, intestine, spleen, head kidney, and blood with Ploy I:C, LPS, PGN, and *P. plecoglossicida* stimulation were assayed by qRT-PCR analysis. The results showed that *Lc*-TRIF was significantly induced upon LPS challenge in mucosal immune tissues (gill and intestine), peripheral immune organ/tissue (spleen and head kidney), and peripheral blood, which was 4.7- and 3.1-fold increase at 3 and 6 hpi in gill (Fig. 8A), 2.3-fold increase at 3 hpi in intestine (Figs. 8B), 7.6- and 2.9-fold increase at 6 hpi in spleen and head kidney (Fig. 8C and D), and with the highest expression level of 9.1-fold increase at 6 hpi in peripheral blood (Fig. 8E). *Lc*-TRIF was also upregulated under poly I:C stimulation, with an approximate 3.6-fold increase at 3 hpi in gill (Figs. 8A), 3.0-fold increase at 6 hpi in intestine (Figs. 8B), 3.3- and 3.4-fold increase at 6 and 12 hpi in peripheral blood (Fig. 8E). In addition, the expression level of *Lc*-TRIF was also increased in response to *P. plecoglossicida* infection, with 2.5-fold at 3 hpi in intestine (Figs. 8B), 4.2-fold at 6 hpi in spleen (Figs. 8C), 6.6-fold at 12 hpi in head kidney (Figs. 8D), 5.7-fold at 6 hpi in peripheral blood (Fig. 8E), and PGN stimulation also initiated significantly up-regulation of *Lc*-TRIF, with 4.6-fold at 3 hpi in intestine (Figs. 8B), and 2.9-fold at 6 hpi in peripheral blood (Fig. 8E). Nevertheless, a significantly down-regulation was found at 3 hpi under poly I:C stimulation in spleen and head kidney (Fig. 8C and D), and such down-regulation could also been found at 24 hpi under the challenge of LPS and *P. plecoglossicida* in intestine, spleen, head kidney and peripheral blood (Fig. 8B, C, D, and E).

3.6. Activation of NF-κB, IFN1, IRF3, and IRF7 promoter by Lc-TRIF

In order to understand whether *Lc*-TRIF could function in the activation of NF-κB and the production of type I IFN, *Lc*-TRIF expression plasmid pcDNA3.1-TRIF together with NF-κB or type I IFN reporter plasmid were co-transfected into HEK 293T cell and then detected by luciferase assays. The results showed that overexpression of *Lc*-TRIF provoke a strong activation of NF-κB promoter in a plasmid dose-dependent manner, being up to 547.7-fold increase relative to pcDNA3.1 vector control at a dose of 200 ng plasmids, and 18.7-fold increase at 5 ng (Fig. 9A). The overexpression of *Lc*-TRIF also initiated the induction of type I IFN promoter, with the peak value of 2.8-fold higher than the control when transfection amount was 50 ng, however, with the transfection amount went higher, the induction level down-regulated, which was 2.3-fold increase relative to the control (Fig. 9B).

Additionally, it was also revealed that overexpression of *Lc*-TRIF could significantly induce the activation of large yellow croaker IRF3 and IRF7 promoter (Fig. 9C and D), and such induction was also in a dose-dependent manner, being up to 7.0-fold increase compared to the control when transfection amount was 200 ng in the assay of IRF3 promoter activity (Figs. 9C), and 2.2-fold higher relative to the control when transfection amount was 200 ng in the detection of IRF7 promoter activity (Fig. 9D). These results suggested that *Lc*-TRIF could facilitate IRF3- and IRF7-mediated signaling pathway in host immune response.

4. Discussion

As the first report described in 2002, TRIF has been identified as a third adaptor harboring the TIR domain that functions downstream of mammalian TLR3 and TLR4, initiating the host antiviral as well as proinflammatory response by activating IFN-β and NF-κB [31]. Whereas in teleost fish, TRIF ortholog was first identified in channel catfish [14], together with the findings that bony fish have several

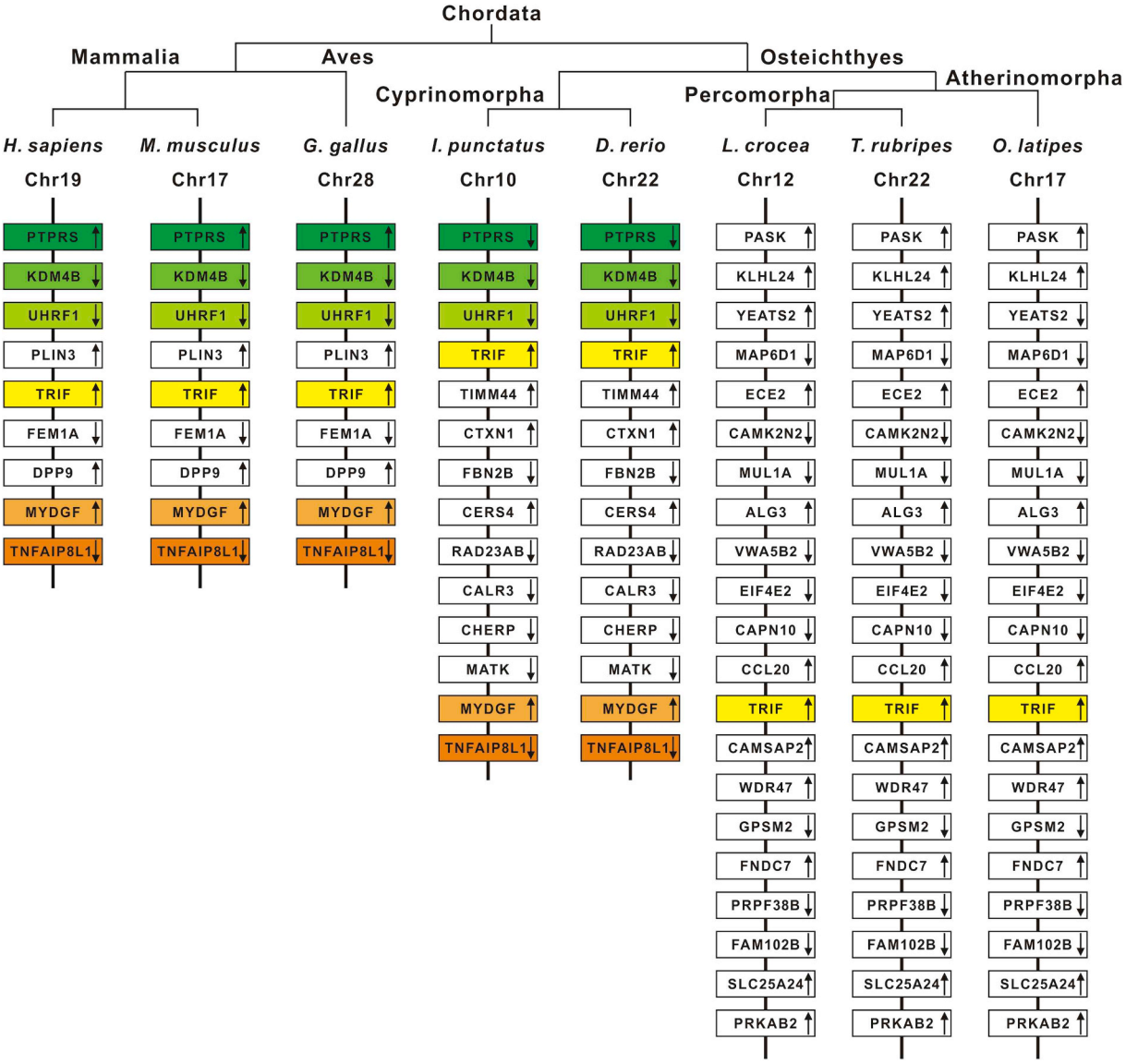

Fig. 4. Gene syntenic mapping of TRIF loci in vertebrates. Conserved genes are boxed, and vertical lines represent chromosome, arrows symbols indicate the gene transcription direction. TRIF is marked with yellow. UHRF1, KDM4B and PTPRS are illustrated in light, middle, and dark green, whereas MYDGF and TNFAIP8L1 are indicated in light orange and orange, respectively. Abbreviations for genes used in this figure: PTPRS, protein tyrosine phosphatase, receptor type S; KDM4B, lysine demethylase 4B; UHRF1, ubiquitin like with PHD and ring finger domains 1; PLIN3, perilipin 3; TRIF, TIR-domain-containing adapter-inducing interferon-β; FEM1A, fem-1 homolog A; DPP9, dipeptidyl peptidase 9; MYDGF, myeloid derived growth factor; TNFAIP8L1, TNF alpha induced protein 8 like 1; TIMM44, translocase of inner mitochondrial membrane 44 homolog (yeast); CTXN1, cortexin 1; FBN2B, fibrillin 2b; CERS4, ceramide synthase 4; RAD23AB, RAD23 homolog A, nucleotide excision repair protein b; CALR3, calreticulin 3; CHERP, calcium homeostasis endoplasmic reticulum protein; MATK, megakaryocyte-associated tyrosine kinase; PASK, PAS domain containing serine/threonine kinase; KLHL24, kelch-like family member 24; YEATS2, YEATS domain containing 2; MAP6D1, MAP6 domain containing 1; ECE2, endothelin converting enzyme 2; CAMK2N2, calcium/calmodulin dependent protein kinase II inhibitor 2; MUL1A, mitochondrial E3 ubiquitin protein ligase 1a; ALG3, asparagine-linked glycosylation 3; VWA5B2, von Willebrand factor A domain containing 5B2; EIF4E2, eukaryotic translation initiation factor 4E family member 2; CAPN10, calpain 10; CCL20, chemokine (C–C motif) ligand 20; CAMSAP2, calmodulin regulated spectrin-associated protein family, member 2; WDR47, WD repeat domain 47; GPSM2, G protein signaling modulator 2; FNDC7, fibronectin type III domain containing 7; PRPF38B, pre-mRNA processing factor 38B; FAM102B, family with sequence similarity 102, member B; SLC25A24, calcium-binding mitochondrial carrier protein SCaMC-1; PRKAB2, 5′-AMP-activated protein kinase subunit beta-2. (For interpretation of the references to colour in this figure legend, the reader is referred to the Web version of this article.)

"fish-specific" TLRs [7,8], and that fugu TLR22 along with TLR3 can trigger TRIF in the immune signaling cascade [17,20], collectively implying that fish TRIF has an important function in fish immune defense. In the current study, a novel teleost TRIF gene was characterized in large yellow croaker, named *Lc*-TRIF. It was found that although the genome structure of TRIF was conserved in vertebrates, the protein sequences exhibit much lower conservation, with *Lc*-TRIF shares 33% amino acid similarity with its human counterpart. Expression analysis indicated that *Lc*-TRIF was expressed in various organs/tissues, and could be induced under challenge of different PAMPs. Notably, *Lc*-TRIF expression could significantly induce the activation of NF-κB, IFN1, IRF3, and IRF7 promoters, suggesting that *Lc*-TRIF functions in host

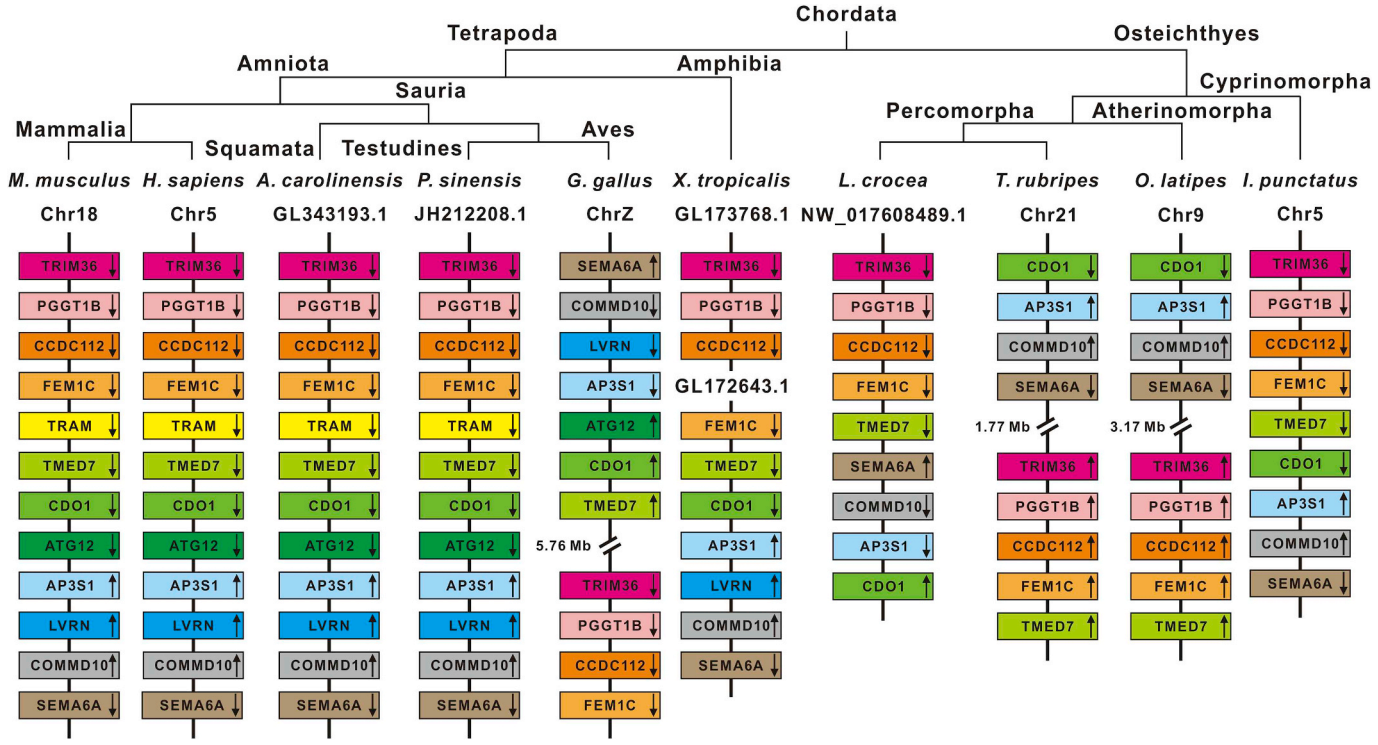

Fig. 5. Gene syntenic mapping of TRAM loci in vertebrates. Conserved genes are boxed, and vertical lines represent chromosome, arrows symbols indicate the gene transcription direction. TRAM is marked with yellow, whereas FEM1C and CCDC112 are indicated in light orange and orange, respectively. PGGT1B and TRIM36 are illustrated in pink and magenta, respectively. TMED7, CDO1, and ATG12 are dyed in light, middle and dark green, AP3S1 and LVRN are indicated in light blue and blue, whereas COMMD10 and SEMA6A are marked using gray and brown, respectively. Abbreviations for genes used in this figure: TRIM36, tripartite motif containing 36; PGGT1B, protein geranylgeranyltransferase type I subunit beta, CCDC112, coiled-coil domain containing 112; FEM1C, fem-1 homolog C; TRAM, TRIF-related adaptor molecule; TMED7, transmembrane p24 trafficking protein 7; CDO1, cysteine dioxygenase type 1; ATG12, autophagy related 12; AP3S1, adaptor related protein complex 3 subunit sigma 1; LVRN, laeverin; COMMD10, COMM domain containing 10; SEMA6A, semaphorin 6A. (For interpretation of the references to colour in this figure legend, the reader is referred to the Web version of this article.)

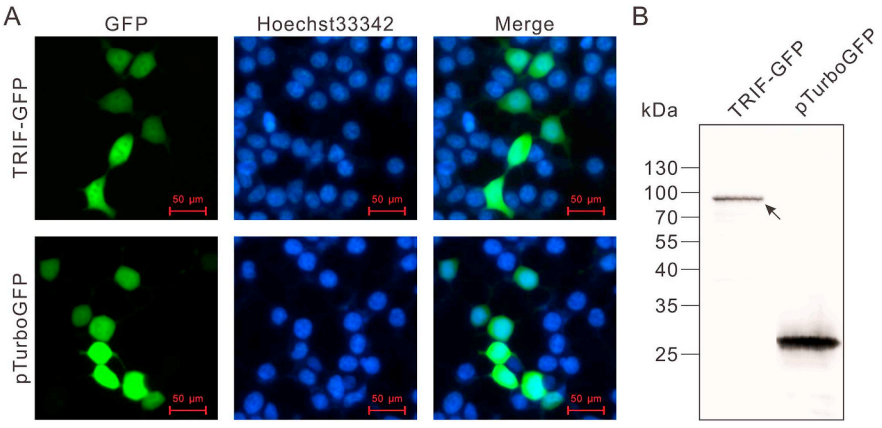

Fig. 6. Subcellular localization of *Lc*-TRIF in HEK 293T cells. (A) HEK 293T cells were transiently transfected with pTurboGFP and pTurbo-TRIF-GFP, respectively. 24 h post-transfection, the nucleus was stained with Hoechst 33342 and the cells were detected and photographed under a fluorescent microscope. (B) The expression of TRIF-GFP and pTurboGFP fusion proteins were confirmed by western blotting analysis using *anti*-TurboGFP antibody.

immune response via NF-κB-, and also IRF3/7-mediated signaling pathway.

Lc-TRIF was constitutively expressed in all the tested organs/tissues in healthy large yellow croaker, with the highest expression in gill. Similar studies in other teleost fish also revealed the constitutively expression of TRIF in various tissues, but the expression pattern was different from various species, with the highest expression level in ovary of channel catfish [14], liver of zebrafish [16], foregut of grass carp [18], and intestine of grouper [19], respectively. Notably, it has been revealed in large yellow croaker that lots of immune-related gene

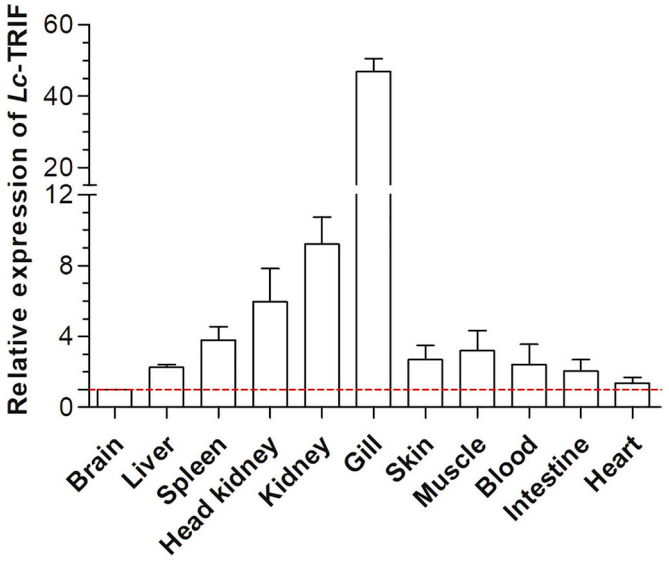

Fig. 7. Organs/tissues distribution analysis of *Lc*-TRIF in healthy large yellow croaker. The mRNA expression levels of *Lc*-TRIF were examined in 11 various organs/tissues of healthy fish (N = 6) by qRT-PCR, with normalizing to the expression of β-actin. The expression level of *Lc*-TRIF in brain was set as 1-fold, with the expression level in other organs/tissues recorded as fold relative to that in brain, and the base line of 1-fold was marked with red dotted line. All data is shown as mean ± SE (N = 6). (For interpretation of the references to colour in this figure legend, the reader is referred to the Web version of this article.)

highly expressed in gill [32–34], and gill-associated lymphoid tissue (GIALT) along with gut-associated lymphoid tissue (GALT) and skin-associated lymphoid tissue (SALT) compose the mucosa-associated lymphoid tissue (MALT) in teleost fish [35], suggesting *Lc*-TRIF may exert functions in mucosa immunity against pathogenic invasion. Additionally, the expression level of *Lc*-TRIF was significantly induced under poly I:C, LPS, PGN, and *P. plecoglossicida* stimulation in gill, intestine, spleen, head kidney, and blood, although such expression change were differ from various stimulations and organs/tissues. A previous study on the transcriptome analysis in spleen revealed that *Lc*-TRIF could be induced by poly I:C stimulation [36]. Studies in other teleost fish also revealed that zebrafish TRIF was significantly induced by PGN, Zymosan, and Glucan stimulation [16], grass carp TRIF was up-regulation in spleen and head kidney in response to grass carp reovirus (GCRV) infection [18], and grouper TRIF was significantly modulated in spleen by poly I:C and LPS challenge [19]. These data collectively indicate that teleost fish TRIF may exhibit extraordinarily broad roles in host innate immune system, with function in host antiviral as well as antibacterial response.

It has been demonstrated that in mammals TRIF could induce NF-κB and IFN-β [37,38]. And the activation of NF-κB of TRIF-dependent pathway has been determined that was through the recruitment of TRAF6 and RIP1 by its TRAF6 binding motif and C-terminal RHIM domain, respectively [38–41]. However, it was noteworthy that *Lc*-TRIF lack the apparent TRAF6 binding motif, and the C-terminal RHIM domain was not that conserved as that found in mammals, since some of the conserved amino acid sites were absent [40], although the core motif (I/V)Q(I/L/V)G*XXNX*(M/L/I) mentioned in a previous report [42] exhibited a relatively conservation. Intriguingly, *Lc*-TRIF expression significantly induce the activation of NF-κB, even when the transfection amount was as little as 5 ng, implying the conserved function of *Lc*-TRIF in NF-κB-mediating signaling cascade. Similar investigation in teleost fish also revealed that fish TRIF was capable in activating NF-κB [15,16,19], although zebrafish TRIF-mediated NF-κB activation was in a different manner, which was down-regulated as the transfected TRIF plasmid went higher of the initial up-regulation by 200 ng TRIF plasmid [16]. Additionally, studies in zebrafish also revealed that TRIF could interact with RIP1 but not TRAF6, and mutation of TRIF RHIM domain disrupted NF-κB activation [15], suggesting that fish TRIF-mediating NF-κB activation was via the association with RIP1, which was differ from that found in mammals.

Studies in mammals have demonstrated that TRIF-mediated IFN-β production is via the association of TRIF-TBK1 through TBK1 binding motif [38,43], which has been defined as a protein motif (GCSLRSTGSP) in human, with Leu^{194} function indispensable for TRIF-mediated IRF3 activation, in which Leu^{194} is critical for recruitment of TBK1 [43]. Multiple alignment data of the protein sequences presented herein showed TBK1 binding motif mentioned above was not that conserved in vertebrates as that found in human, but a conserved Leu was exist in all the examined species. Meanwhile, *Lc*-TRIF was capable in the activation of type I IFN, together with the previous findings that other teleost TRIF function in inducting IFN promoter activation [15,16,19], and zebrafish TRIF could interact with TBK1 [15], collectively suggesting the conserved TRIF-TBK1 signaling cascade in teleost fish. In particular, it was for the first time, to our knowledge, revealed that fish TRIF significantly inducing IRF3 as well as IRF7 promoter activity, indicating that fish IRF3- and IRF7-dependent signaling pathway are involved in TRIF-mediated induction of type I IFN, although the mechanism remain needs more study, especially TRIF-IRF7-dependent signaling cascade. It should be noted that a previous study in zebrafish presented a surprising finding that a TRIF construct lacking the N-terminal domain (1–311 aa), which was essential for interaction with TBK1, exhibited an enhanced activation of type I IFN promoter, and mutation of the RHIM domain resulted in diminished capacity in IFN activation [15], suggesting that TBK1-mediated signaling cascade was not the only pathway that TRIF recruited in activation of type I IFN production, other adaptors such as RIP1-dependent mechanism may participate in the IFN activation. Recent studies also revealed that N-terminal domain of mammalian TRIF (1–153 aa) could form an intramolecular interaction with the TIR domain, acting as an auto-regulator that prevent downstream signaling molecules from accessing TRIF and suppress activation of IFN-β and NF-κB [43–45], which could also be an explanation for enhancement of type I IFN activation in zebrafish TRIF without N-terminal domain.

TRAM, a fourth adaptor characterized in TLR signaling pathway, has been determined as a bridging adaptor function exclusively in TLR4 pathway through interacting with TRIF [11,37,46]. Comprehensive analyses of synteny and phylogeny from representative species of the vertebrate classes in the present study confirmed a hypothesis proposed previously that TRAM is not exist in fish, which makes fish more resistant to endotoxic shock [47]. It has been shown in the present research that FEM1C and TMED7 are flanking genes of TRAM in mammals and reptiles, whereas FEM1C and TMED7 maintained adjacent to each other but without TRAM been found between them in fish, amphibians or birds, although FEM1C and TMED7 exhibited a long distance from each other in the chicken genome, which may due to the unreasonable genome sequencing and mapping [15]. Additionally, evolutionary analysis based on protein sequence comparison also indicated that TRIF and TRAM evolved from the same ancestor after an

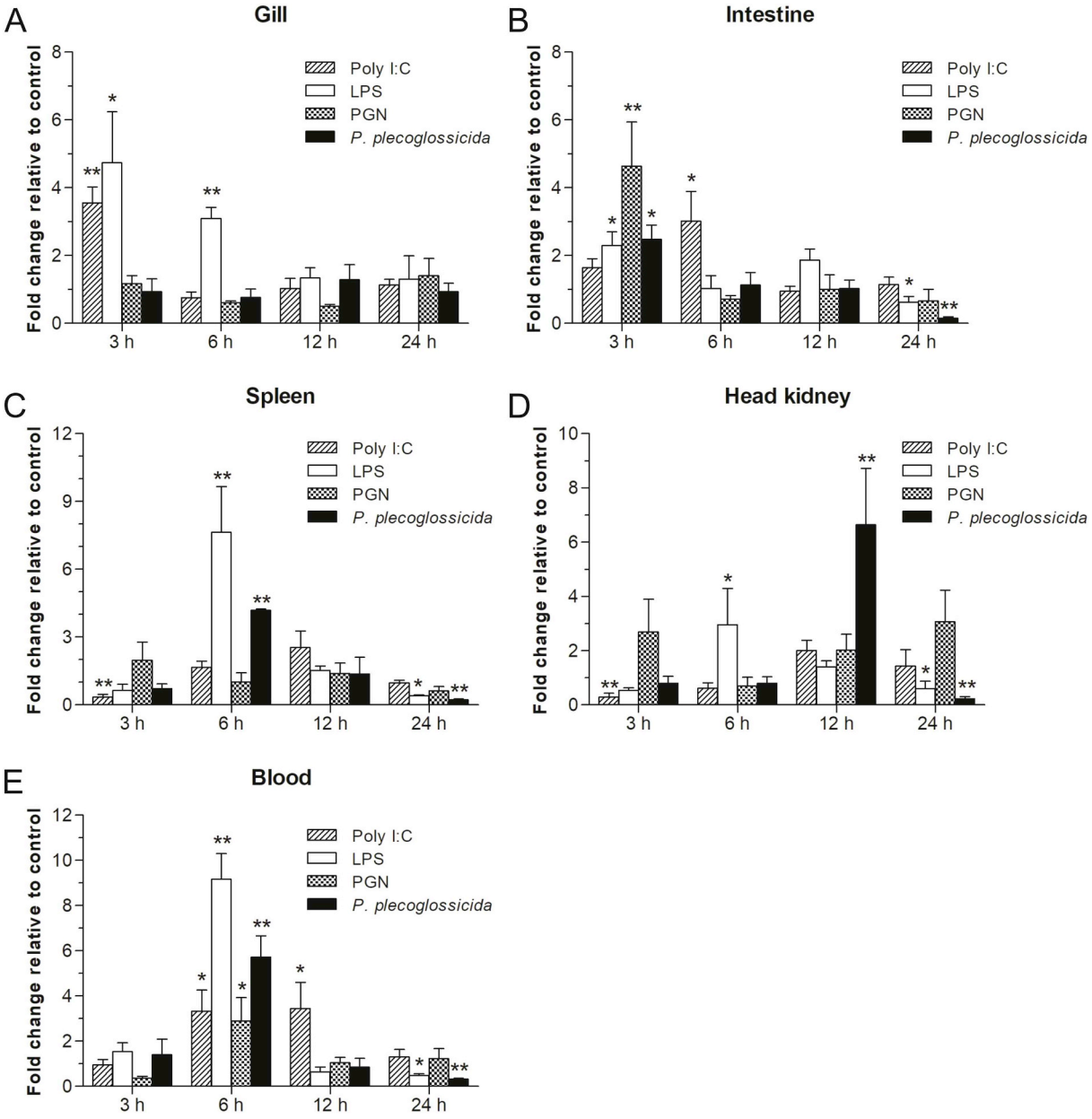

Fig. 8. Expression analysis of *Lc*-TRIF under stimulation of poly I:C, LPS, PGN, and *P. plecoglossicida*. The healthy large yellow croaker was divided into five groups and then injected intraperitoneally with 100 μl of poly I:C (1 mg/ml), LPS (0.5 mg/ml), PGN (1 mg/ml), *P. plecoglossicida* suspension in PBS (5×10^5 CFU/ml) and PBS (control), respectively. The mRNA expression levels of *Lc*-TRIF in fish gill (A), intestine (B), spleen (C), head kidney (D) and blood (E) were detected by qRT-PCR at 3, 6, 12, and 24 h post stimulation. The expression level changes were calculated by normalization to the expression of β-actin and then recorded as fold induction compared with PBS injection group (control) at the same time point. All of the data is shown as mean ± SE (N = 6), with bars representing SE. $^*P < 0.05$, $^{**}P < 0.01$.

early gene duplication event and then divided into two branches in higher vertebrates. It is therefore hypothesized that TRAM may be lost after the divergence of rayfin and lobfin fishes 450 million years ago [15,16,47]. Particularly, it has been determined that "fish-specific" TLRs including TLR19, TLR20, TLR21, TLR22, and TLR23 are exist in teleost fish [7,8], and fugu TRIF act as the adaptor of TLR22 as well as TLR3 [17,20]. So far, the adaptors function downstream such TLRs remain poorly understand. Is it the fact that fish only employ MyD88, TIRAP, TRIF, and SARM as adaptors to perform TLR-mediated signaling pathway? Do there still exist some TLR adaptors that we have not characterized? Taken together, it is of great importance for the future investigation to identify the downstream factors that play important roles in fish TLR signaling cascade which is essential in understanding TLR signaling in fish and also uncover more in depth functional similarities and divergences as that in mammals.

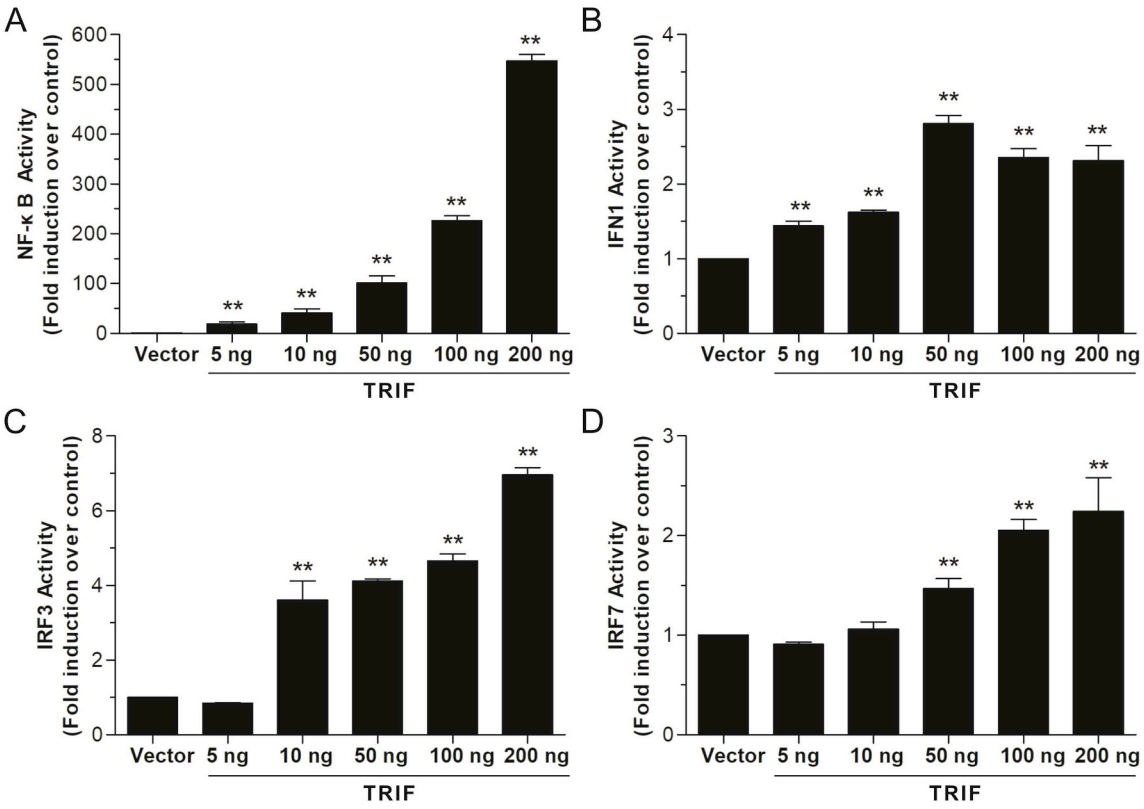

Fig. 9. Activation of NF-κB, IFN1, IRF3, and IRF7 response by *Lc*-TRIF. (A) Induction of NF-κB promoter activity by *Lc*-TRIF. (B) Induction of IFN1 promoter activity by *Lc*-TRIF. (C) Induction of IRF3 promoter activity by *Lc*-TRIF. (D) Induction of IRF7 promoter activity by *Lc*-TRIF. HEK 293T cells seeded in 24-well plates were cotransfected with 100 ng of pNF-κB-luc, pGL4-IFN1-pro, pGL4-IRF3-pro or pGL4-IRF7-pro, 10 ng pRL-TK together with various amounts of pcDNA3.1-TRIF or pcDNA3.1 as control. At 24 h post-transfection, the cells were harvested for the detection of luciferase activity. Data were expressed as mean ± SE from three independent experiments, with bars representing SE. $*P < 0.05$, $**P < 0.01$.

Acknowledgements

This work was supported by the National Natural Science Foundation of China (Grant No. 31772878 and 31402273), the Natural Science Foundation of Fujian Province of China (No. 2018J06008 and 2017J05055), and "Program for Excellent Young Talents in Fujian Province University".

Appendix A. Supplementary data

Supplementary data to this article can be found online at https://doi.org/10.1016/j.fsi.2019.05.011.

References

[1] E. Meylan, J. Tschopp, M. Karin, Intracellular pattern recognition receptors in the host response, Nature 442 (7098) (2006) 39–44.
[2] T.H. Mogensen, Pathogen recognition and inflammatory signaling in innate immune defenses, Clin. Microbiol. Rev. 22 (2) (2009) 240–273.
[3] T. Kawai, S. Akira, The roles of TLRs, RLRs and NLRs in pathogen recognition, Int. Immunol. 21 (4) (2009) 317–337.
[4] T. Kawai, S. Akira, The role of pattern-recognition receptors in innate immunity: update on Toll-like receptors, Nat. Immunol. 11 (5) (2010) 373–384.
[5] H. Kumar, T. Kawai, S. Akira, Pathogen recognition by the innate immune system, Int. Rev. Immunol. 30 (1) (2011) 16–34.
[6] S.W. Brubaker, K.S. Bonham, I. Zanoni, J.C. Kagan, Innate immune pattern recognition: a cell biological perspective, Annu. Rev. Immunol. 33 (2015) 257–290.
[7] A. Rebl, T. Goldammer, H.M. Seyfert, Toll-like receptor signaling in bony fish, Vet. Immunol. Immunopathol. 134 (3–4) (2010) 139–150.
[8] Y. Palti, Toll-like receptors in bony fish: from genomics to function, Dev. Comp. Immunol. 35 (12) (2011) 1263–1272.
[9] K.A. Jenkins, A. Mansell, TIR-containing adaptors in Toll-like receptor signalling, Cytokine 49 (3) (2010) 237–244.
[10] T. Ve, N.J. Gay, A. Mansell, B. Kobe, S. Kellie, Adaptors in toll-like receptor signaling and their potential as therapeutic targets, Curr. Drug Targets 13 (11) (2012) 1360–1374.
[11] L.A. O'Neill, A.G. Bowie, The family of five: TIR-domain-containing adaptors in Toll-like receptor signalling, Nat. Rev. Immunol. 7 (5) (2007) 353–364.
[12] M.O. Ullah, M.J. Sweet, A. Mansell, S. Kellie, B. Kobe, TRIF-dependent TLR signaling, its functions in host defense and inflammation, and its potential as a therapeutic target, J. Leukoc. Biol. 100 (1) (2016) 27–45.
[13] J. Hyun, S. Kanagavelu, M. Fukata, A unique host defense pathway: TRIF mediates both antiviral and antibacterial immune responses, Microb. Infect. 15 (1) (2013) 1–10.
[14] P. Baoprasertkul, E. Peatman, B. Somridhivej, Z.J. Liu, Toll-like receptor 3 and TICAM genes in catfish: species-specific expression profiles following infection with *Edwardsiella ictaluri*, Immunogenetics 58 (10) (2006) 817–830.
[15] C. Sullivan, J.H. Postlethwait, C.R. Lage, P.J. Millard, C.H. Kim, Evidence for evolving Toll-IL-1 receptor-containing adaptor molecule function in vertebrates, J. Immunol. 178 (7) (2007) 4517–4527.
[16] S. Fan, S.W. Chen, Y.H. Liu, Y.Q. Lin, H. Liu, L. Guo, B. Lin, S.F. Huang, A.L. Xu, Zebrafish TRIF, a golgi-localized protein, participates in IFN induction and NF-kappa B activation, J. Immunol. 180 (8) (2008) 5373–5383.
[17] A. Matsuo, H. Oshiumi, T. Tsujita, H. Mitani, H. Kasai, M. Yoshimizu, M. Matsumoto, T. Seya, Teleost TLR22 recognizes RNA duplex to induce IFN and protect cells from birnaviruses, J. Immunol. 181 (5) (2008) 3474–3485.
[18] C.R. Yang, Q.M. Li, J.G. Su, X.H. Chen, Y.P. Wang, L.M. Peng, Identification and functional characterizations of a novel TRIF gene from grass carp (*Ctenopharyngodon idella*), Dev. Comp. Immunol. 41 (2) (2013) 222–229.
[19] J.G. Wei, X. Zhang, S.Q. Zang, Q.W. Qin, Expression and functional characterization of TRIF in orange-spotted grouper (*Epinephelus coioides*), Fish Shellfish Immunol. 71 (2017) 295–304.
[20] T. Seya, M. Matsumoto, T. Ebihara, H. Oshiumi, Functional evolution of the TICAM-1 pathway for extrinsic RNA sensing, Immunol. Rev. 227 (1) (2009) 44–53.
[21] P.F. Zou, M.X. Chang, Y. Li, S. Huan Zhang, J.P. Fu, S.N. Chen, P. Nie, Higher antiviral response of RIG-I through enhancing RIG-I/MAVS-mediated signaling by its long insertion variant in zebrafish, Fish Shellfish Immunol. 43 (1) (2015) 13–24.
[22] P.F. Zou, M.X. Chang, Y. Li, N.N. Xue, J.H. Li, S.N. Chen, P. Nie, NOD2 in zebrafish functions in antibacterial and also antiviral responses via NF-kappaB, and also MDA5, RIG-I and MAVS, Fish Shellfish Immunol. 55 (2016) 173–185.
[23] P.F. Zou, M.X. Chang, N.N. Xue, X.Q. Liu, J.H. Li, J.P. Fu, S.N. Chen, P. Nie, Melanoma differentiation-associated gene 5 in zebrafish provoking higher interferon-promoter activity through signalling enhancing of its shorter splicing variant,

Immunology 141 (2) (2014) 192–202.
[24] J.T. Zhang, S.M. Zhou, S.W. An, L. Chen, G.L. Wang, Visceral granulomas in farmed large yellow croaker, *Larimichthys crocea* (Richardson), caused by a bacterial pathogen, *Pseudomonas plecoglossicida*, J. Fish Dis. 37 (2) (2014) 113–121.
[25] L. Huang, L. Zhao, Y. Su, Q. Yan, Genome sequence of *Pseudomonas plecoglossicida* strain NZBD9, Genome Announc. 6 (4) (2018), https://doi.org/10.1128/genomeA.01412-17.
[26] Y. Ding, J. Ao, X. Huang, X. Chen, Identification of two subgroups of type I IFNs in Perciforme fish large yellow croaker *Larimichthys crocea* provides novel insights into function and regulation of fish type I IFNs, Front. Immunol. 7 (2016) 343.
[27] A. Marchler-Bauer, Y. Bo, L. Han, J. He, C.J. Lanczycki, S. Lu, F. Chitsaz, M.K. Derbyshire, R.C. Geer, N.R. Gonzales, M. Gwadz, D.I. Hurwitz, F. Lu, G.H. Marchler, J.S. Song, N. Thanki, Z. Wang, R.A. Yamashita, D. Zhang, C. Zheng, L.Y. Geer, S.H. Bryant, CDD/SPARCLE: functional classification of proteins via subfamily domain architectures, Nucleic Acids Res. 45 (D1) (2017) D200–D203.
[28] M.A. Larkin, G. Blackshields, N.P. Brown, R. Chenna, P.A. McGettigan, H. McWilliam, F. Valentin, I.M. Wallace, A. Wilm, R. Lopez, J.D. Thompson, T.J. Gibson, D.G. Higgins, Clustal W and clustal X version 2.0, Bioinformatics 23 (21) (2007) 2947–2948.
[29] S. Kumar, G. Stecher, K. Tamura, MEGA7: molecular evolutionary genetics analysis version 7.0 for bigger datasets, Mol. Biol. Evol. 33 (7) (2016) 1870–1874.
[30] M.W. Pfaffl, A new mathematical model for relative quantification in real-time RT-PCR, Nucleic Acids Res. 29 (9) (2001) 2002–2007.
[31] M. Yamamoto, S. Sato, K. Mori, K. Hoshino, O. Takeuchi, K. Takeda, S. Akira, Cutting edge: a novel Toll/IL-1 receptor domain-containing adapter that preferentially activates the IFN-beta promoter in the Toll-like receptor signaling, J. Immunol. 169 (12) (2002) 6668–6672.
[32] Y. Ding, C. Ai, Y. Mu, J. Ao, X. Chen, Molecular characterization and evolution analysis of five interleukin-17 receptor genes in large yellow croaker *Larimichthys crocea*, Fish Shellfish Immunol. 58 (2016) 332–339.
[33] M. Sun, Y. Mu, Y. Ding, J. Ao, X. Chen, Molecular and functional characterization of Toll-like receptor 21 in large yellow croaker (*Larimichthys crocea*), Fish Shellfish Immunol. 59 (2016) 179–188.
[34] Y. Ding, J. Ao, X. Chen, Comparative study of interleukin-17C (IL-17C) and IL-17D in large yellow croaker *Larimichthys crocea* reveals their similar but differential functional activity, Dev. Comp. Immunol. 76 (2017) 34–44.
[35] I. Salinas, Y.A. Zhang, J.O. Sunyer, Mucosal immunoglobulins and B cells of teleost fish, Dev. Comp. Immunol. 35 (12) (2011) 1346–1365.
[36] Y. Mu, M. Li, F. Ding, Y. Ding, J. Ao, S. Hu, X. Chen, De novo characterization of the spleen transcriptome of the large yellow croaker (*Pseudosciaena crocea)* and analysis of the immune relevant genes and pathways involved in the antiviral response, PLoS One 9 (5) (2014) e97471.
[37] K.A. Fitzgerald, D.C. Rowe, B.J. Barnes, D.R. Caffrey, A. Visintin, E. Latz, B. Monks, P.M. Pitha, D.T. Golenbock, LPS-TLR4 signaling to IRF-3/7 and NF-kappaB involves the toll adapters TRAM and TRIF, J. Exp. Med. 198 (7) (2003) 1043–1055.
[38] S. Sato, M. Sugiyama, M. Yamamoto, Y. Watanabe, T. Kawai, K. Takeda, S. Akira, Toll/IL-1 receptor domain-containing adaptor inducing IFN-beta (TRIF) associates with TNF receptor-associated factor 6 and TANK-binding kinase 1, and activates two distinct transcription factors, NF-kappa B and IFN-regulatory factor-3, in the Toll-like receptor signaling, J. Immunol. 171 (8) (2003) 4304–4310.
[39] Z. Jiang, T.W. Mak, G. Sen, X. Li, Toll-like receptor 3-mediated activation of NF-kappaB and IRF3 diverges at Toll-IL-1 receptor domain-containing adapter inducing IFN-beta, Proc. Natl. Acad. Sci. U. S. A. 101 (10) (2004) 3533–3538.
[40] E. Meylan, K. Burns, K. Hofmann, V. Blancheteau, F. Martinon, M. Kelliher, J. Tschopp, RIP1 is an essential mediator of Toll-like receptor 3-induced NF-kappa B activation, Nat. Immunol. 5 (5) (2004) 503–507.
[41] W.J. Kaiser, M.K. Offermann, Apoptosis induced by the toll-like receptor adaptor TRIF is dependent on its receptor interacting protein homotypic interaction motif, J. Immunol. 174 (8) (2005) 4942–4952.
[42] W.J. Kaiser, J.W. Upton, E.S. Mocarski, Receptor-interacting protein homotypic interaction motif-dependent control of NF-kappa B activation via the DNA-dependent activator of IFN regulatory factors, J. Immunol. 181 (9) (2008) 6427–6434.
[43] M. Tatematsu, A. Ishii, H. Oshiumi, M. Horiuchi, F. Inagaki, T. Seya, M. Matsumoto, A molecular mechanism for Toll-IL-1 receptor domain-containing adaptor molecule-1-mediated IRF-3 activation, J. Biol. Chem. 285 (26) (2010) 20128–20136.
[44] M.O. Ullah, T. Ve, M. Mangan, M. Alaidarous, M.J. Sweet, A. Mansell, B. Kobe, The TLR signalling adaptor TRIF/TICAM-1 has an N-terminal helical domain with structural similarity to IFIT proteins, Acta Crystallogr. Sect. D Biol. Crystallogr. 69 (Pt 12) (2013) 2420–2430.
[45] J. Mahita, R. Sowdhamini, Integrative modelling of TIR domain-containing adaptor molecule inducing interferon-beta (TRIF) provides insights into its autoinhibited state, Biol. Direct 12 (1) (2017) 9.
[46] H. Oshiumi, M. Sasai, K. Shida, T. Fujita, M. Matsumoto, T. Seya, TIR-containing adapter molecule (TICAM)-2, a bridging adapter recruiting to Toll-like receptor 4 TICAM-1 that induces interferon-beta, J. Biol. Chem. 278 (50) (2003) 49751–49762.
[47] D.B. Iliev, J.C. Roach, S. Mackenzie, J.V. Planas, F.W. Goetz, Endotoxin recognition: in fish or not in fish? FEBS Lett. 579 (29) (2005) 6519–6528.